

ASYNCHRONOUS STEREO VISION SYSTEM FOR FRONT-VEHICLE DETECTION

Chung-Cheng Chiu, Wen-Chung Chen, Min-Yu Ku, and Yuh-Jiun Liu

Department of Electrical and Electronic Engineering,
Chung Cheng Institute of Technology, National Defense University,
No. 190, Sanyuan 1st St., Dashi Jen, Taoyuan, 335 Taiwan, R.O.C.
E-mail: davidchiu@ndu.edu.tw

ABSTRACT

This study uses two low-cost and compact CMOS cameras to construct an asynchronous binocular system and proposes an effective real-time front-vehicle detection algorithm with the binocular system. The proposed vehicle detection algorithm uses the edge information to detect the region of each front vehicle, and then computes the disparities of the front vehicles by an adaptive search method. According to the disparity values, the relative distances between the front and the host vehicles can be computed. The proposed algorithm of the manuscript conquers the asynchronous exposure problem and cost issue of a binocular system. Experimental results show that the proposed system can robustly and accurately detect obstacles or other vehicles in real time under different illumination and road conditions.

KEY WORDS : Synchronous stereovision system, Asynchronous stereovision system, Disparity, Obstacle detection.

1. INTRODUCTION

According to the final report of the National Highway Traffic Safety Administration [1], front collision warning systems (FCWS) with existing passive safety equipments on board can effectively reduce rear-end collisions by 21%. Millimeter-wave radar [2] has a good range but its angular resolution is low. Although millimeter-wave radar systems have been used on commercial vehicles [3], they are not suitable for distinguishing obstacles and vehicles in complex urban backgrounds. Laser radar has been used as the sensor in other systems for detecting the environmental information and tracking the moving objects [4]. Although Laser radar costs less than millimeter-wave radar, they have the same limitations as the other radar systems that are unsuitable for classifying obstacles or recognizing lane markings.

By the spatial resolution of the image, vision sensors can operate complex industrial robot to execute the precise robotic maneuver [5] and be suitable for recognizing and tracking the moving obstacles. So far, on-board vision sensors for detecting obstacles can be divided into mono- and stereovision systems. Broggi *et al.* [6] used a monocular image sequence to local and track the vehicle. In addition, a number of reports have also presented mono-vision

algorithms for recognizing leading vehicles and obstacles [7]–[8].

Because the stereovision systems can provide distance measurement as well as obstacle detection, stereovision systems are becoming increasingly popular for advanced driver assistance systems and advanced safety vehicles. The well-known epipolar constraint [9] is generally used to describe the geometric relationships between stereo images.

Bensrhair *et al.* [10] and Toulminet *et al.* [11] used a synchronous image capture system to obtain stereo pair images from two synchronous cameras. As the synchronous stereo pair images satisfy the properties of epipolar geometry, corresponding points in the stereo pair images can be matched in the corresponding horizontal scan lines ($Y_L=Y_R$). Labayrade and Hautière *et al.* [12] have described how a fast disparity space image (DSI) was computed, and then obtained the similarity by collecting, for each image row, the number of matches for each disparity value.

The concept of the similarity in each row of an image pair was used in a vision sensor system that was part of TerraMax [13].

Because the price, size, and complicated setup of previous synchronous stereo camera systems make them unsuitable for real-world applications, this study describes a small and low-cost binocular platform that is easy to set up and overcomes the drawbacks of synchronous stereo camera systems. This study proposes a real-time stereovision obstacle detection algorithm to overcome the problems of computational load and image matching to provide better performance with an asynchronous stereo camera system.

2. FRONT VEHICLE DETECTION ALGORITHM

The proposed algorithm can be divided into two modules: searching module and matching module. Firstly, the aim of the proposed searching module in the proposed algorithm is to locate the probable positions of the vehicles in the right or left image. Then, the matching module of the proposed algorithm takes the results of the searching module to match the corresponding pixels from the stereo image pair. And, the distance of the front vehicle is calculated by the disparity of the corresponding pixel difference between the right and left images. The details of the two modules are described as following.

2.1 Searching module

In order to speed up the searching processing, the input right image is downsampled by a factor of 2^n to reduce computational complexity. The image is downsized by a factor of 2, $n=1$, in the x and y directions. After the image is downsized, the Sobel edge detection is used for detecting the horizontal/vertical edge points and the connected-component labeling is used to assemble these edge points into horizontal/vertical line segments.

2.1.1 Find the region of interesting (ROI)

Because the horizontal line segments near the bottom of the image indicates the line segments approaching the host vehicle, the proposed algorithm would take them as the higher threat level. According to the definition of the threat level, the position of each horizontal line segment decides its processing order. We use a near-to-far strategy to sort the seed lines and find the ROI from the bottom row to the top row of the input image.

Firstly, each horizontal line segment is defined as the candidate of a seed line and its length and position are computed. Then, each horizontal line segment is matched by seed lines from the bottom to the top row of the input image to find the ROI. The horizontal line segment belongs to the ROI of a seed line is defined by Eq. (1).

$$|SL_{x1} - IL_{x1}| < Th, |SL_{x2} - IL_{x2}| < Th, \text{ and } SL_y > IL_y, \quad (1)$$

where SL_{x1} is the left point of the seed line, SL_{x2} is the right point of the seed line, IL_{x1} is the left point of the input horizontal line segment, IL_{x2} is the right point of the input horizontal line segment, and SL_y and IL_y are the y -coordinates (vertical direction) of the seed line and input horizontal line segment respectively.

2.1.2 Refine the ROI

The ROI may retain some errors caused by shadows on the surface of the road. The shadows usually expand the range of ROI to cause errors and time-consuming in the matching process. Therefore, we count the edge pixels in the ROI to determine edge symmetries from the horizontal and vertical projection histograms to delete the interference of the shadows in the ROI, shown as Fig. 1.

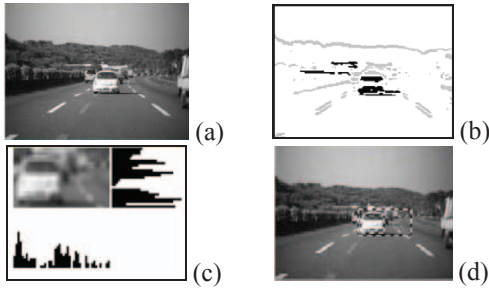


Fig.1 Refine the ROI

In Fig. 1, the Fig. 1(a) is the original input right image; Fig. 1(b) is the edge detections of the right images; Fig. 1(c) is the horizontal and vertical projection histograms of the

ROI which is affected by shadows; Fig. 1(d) is the refined ROI inside the ROI.

2.2 Matching module

After the ROI of the front vehicles have searched in the right image, each extreme pixel of the line segments in the ROI is matched in the left image to find the corresponding pixel in order to calculate the disparity of the corresponding pixel. In order to speed up and reduce the matching error, the matching module proposes zero-mean *SAD* full searching, adaptive shifting of the searching area, and tracking detection to solve the illumination, asynchronous exposure, and tracking problems.

2.2.1 Zero-mean *SAD* full searching

In the asynchronous binocular cameras system, the exposures are independent. And, the gray differences between different corresponding pixels in stereo pair images are fixed. Hence, the snapped right and left images must be equalized in the gray value before the search processing to avoid the influence of exposure.

Assume the block size is $N \times N$, $RC(x, y)$ and $LR(x, y)$ are the image pixel in the right and left image respectively, and $2p$ is the size of the searching window. In the proposed zero-mean *SAD* full searching, the searching method is defined as Eq. (2).

$$SADV(i, j) = \sum_{k=-(N/2)}^{N/2} \sum_{l=-(N/2)}^{N/2} |(RC(x+k, y+l) - M_R) - (LR(i+x+k, j+y+l) - M_L)|$$

$$M_R = \frac{1}{N \times N} \sum_{i=-(N/2)}^{N/2} \sum_{j=-(N/2)}^{N/2} RC(i, j), \text{ and}$$

$$M_L = \frac{1}{N \times N} \sum_{i=-(N/2)}^{N/2} \sum_{j=-(N/2)}^{N/2} LR(i, j), \quad -p \leq i, j \leq p, \quad (2)$$

where the M_R is the mean value of the matching block in the right image and the M_L is the mean value of the matching block in the left image.

2.2.2 Adaptive shifting of the searching area

Because of the asynchronous exposure and the vehicle's vibration, each corresponding pixel can not be matched on the same row in each stereo image pair. However, the shifting of these corresponding pixels is very close in a stereo image pair. Hence, the proposed algorithm can auto-adjust the shifting of the searching area in the left image to reduce the matching time. The proposed system calculates the average shifting of matched pixels to auto-adjust the area of the matching window in ROI. In the experimental results, the proposed adaptive searching area can effectively reduce 50% of CPU consumption in the matching process.

2.2.3 Tracking detection

According to the continuity in the sequence of image frames, the same vehicle in the next frame could be found in the vicinity of the location in the current frame. Therefore,

the tracking detection expands the size of the ROI in the current frame to track the vehicle in the next frame. If the ROI is near the bottom of the input image, the tracking detection expands a larger scale ROI in the next frame; in other words, if the ROI is far from the bottom of the input image, the tracking detection gives a smaller scale ROI in the next frame. Therefore, the proposed algorithm is directly to match the disparity of the vehicle in the next frame illustrated as Fig.2.

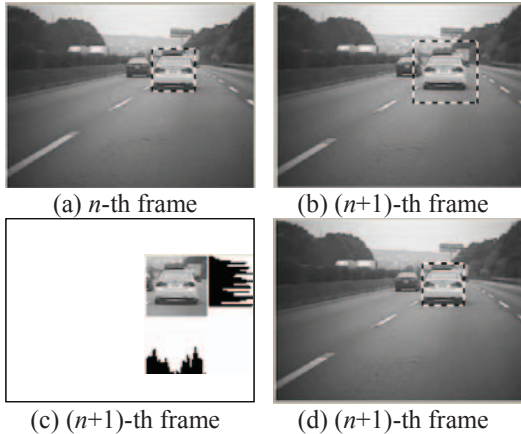


Fig.2 (a) the vehicle has been matched in the n -th frame; (b) expand the original ROI in the $(n+1)$ -th frame; (c) the horizontal and vertical projection histogram of the expanding ROI in the $(n+1)$ -th frame; (d) the vehicle has been tracked in the $(n+1)$ -th frame.

3. EXPERIMENTAL RESULTS

The proposed system is divided into four components: low-cost CMOS camera $\times 2$, USB grabber, and notebook. Figure 3 is the setup of the proposed binocular platform. The hardware of the notebook is a Pentium IV 1.8 GHz. The focal length of CMOS camera is 12 mm and the image size is 320×240 pixels. The program is compiled with the Microsoft Visual C++. The average processing time for each stereo-image pair is approximately 12 to 10 msec, and the frame rate is capable of exceeding 90 fps with NTSC encoding. Thus, the proposed system can be considered a real-time application.



Fig. 3 Setup of the proposed binocular platform

The proposed system has been tested on several roads (i.e. urban road, country path) with respect to different weather and lighting conditions. The detection rates of our system are summarized in Table I for these various conditions.

The detection rate is defined as the percentage of front vehicles detected correctly in the detection zone (4–50 m in the front of the host vehicle). In these tests, the host vehicle maintains a speed of 30–50 km/h to verify the proposed system on the urban road. All of the front vehicles in the test images are selected randomly without prior planning.

Table I Detection rates under different conditions

Weather	Sun	Cloud	Rainy	Night	Total
False/	448/	835/	1000/	2962/	5245/
Detected	32,000	26,342	6,945	16,550	81,837
Detection Rate	98.6%	96.8%	85.6%	82.1%	93.6%

a. Sunny day:

In Fig. 4, the host and front vehicles are on the intersection of urban road. In the complex background, the system can still track the vehicles which enter the detection zone of the proposed system at the same time. In the Fig. 5, the proposed system can detect the vehicles on the two way traffic lane at the same time. The detection rate during the sunny test images is 98.6%.



Fig. 4 Detection on the intersection



Fig. 5 Detection on the two way traffic lane

b. Cloudy day:

The detection rate for the cloudy test images was approximately 96.8%. Although the complex background mixes with the edge of vehicle in Fig. 6, the proposed system can still detect the front vehicles. In the cloudy day, it is interesting to note that the dark vehicle in the front, despite the color is similar to the asphalt road surface such as the left vehicle in Fig. 7, would not affect the correctness of the detection rate in the proposed system.

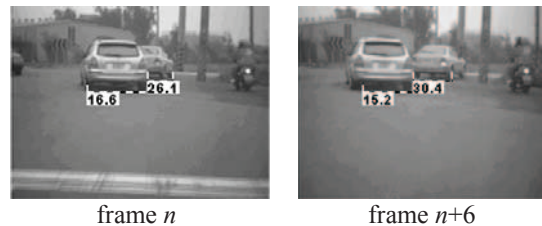


Fig. 6 Detection for occlusion vehicles



frame n frame $n+6$

Fig. 7 Detection for dark vehicles

c. Rainy day:

In the rainy day, the major false detection is the influences from the water on the road surface and the water on the windscreen. The oscillating windscreen wipers wouldn't affect the detection results in the rainy. The detection rate for the rainy test images was approximately 85.6%. Some experimental results are shown in Fig. 8.



frame n frame $n+1$

Fig. 8 Detection on rainy day

d. Night:

The detection rate of the proposed system dropped to 82.1% at night. The night circumstance is the most complex problem of the test sequences. The unexpected light sources cause false detection, such as headlights and tail lights that appeared suddenly. The line segments of the vehicles are disrupted by these spots of light. Figure 9 shows some detection results on the urban road at night.



frame n frame $n+1$

Fig. 9 Detection on night

4. CONCLUSIONS

This manuscript proposes a compact, low-cost and asynchronous binocular platform and an effective real-time front-vehicle detection algorithm. In the experimental results describe the proposed stereovision system for detecting obstacles under various road and illumination conditions. For the real-time applications, the average processing time of the proposed algorithm is approximately 12 to 10 msec, and the frame-processing rate is capable of exceeding 90 fps with NTSC format. Thus the proposed system can be considered to real-time application. Because

of the price, size, and easy setup of the proposed binocular system, the proposed system is suitable for real world applications. The experimental results obtained with various test images show that the proposed system can successfully detect the front vehicles and estimate their distances under various illumination and road conditions.

Acknowledgments

The authors acknowledge financial support from the National Science Council in the form of grant NSC 97-2752-E-009-003-PAE.

REFERENCES

- [1] Gregory M. Fitch, Hesham A. Rakha, Mazen Arafeh, Myra Blanco, Santosh K. Gupta, Richard P. Zimmermann, and Richard J. Hanowski, "Safety Benefit Evaluation of a Front Collision Warning System," Tech. Rep. DOT HS 810 910, NHTSA, U. S. DOT, Feb. 2008.
- [2] K. Kaliyaperumal, S. Lakshmanan, and K. Kluge, "An algorithm for detecting roads and obstacles in radar images" *IEEE Trans. Vehicular Technology*, vol. 50, no. 1, pp. 170 – 182, Jan. 2001.
- [3] S. Yamano, H. Higashida, M. Shono, S. Matsui, T. Tamaki, H. Yagi, and H. Asanuma, "76GHz millimeter wave automobile radar using single chip MMIC," Fujitsu Ten Technical Report, no.23, pp.12–19, 2004.
- [4] C. Castejón, D. Blanco, and L. Moreno, "Compact modeling technique for outdoor navigation" *IEEE Trans. on Systems, Man, and Cybernetics—part a: systems and humans*, vol. 38, no. 1, pp.9–24, Jan. 2008.
- [5] A. Loredó-Flores, E. J. Gonz'alez-Gal'van, J. J. Cervantes-S'anchez, and A. Mart'inez-Soto, "Optimization of industrial, vision-based, intuitively generated robot point-allocating tasks using genetic algorithms" *IEEE Trans. on Systems, Man, and Cybernetics—part c: applications and reviews*, vol. 38, no. 4, pp.600–608, July 2008.
- [6] A. Broggi, M. Bertozzi, A. Fascioli, C. G. L. Bianco, and A. Piazza, "Visual perception of obstacles and vehicles," *IEEE Trans. on Intelligent Transportation Systems*, vol. 1, no. 3, pp. 164 – 176, September 2000.
- [7] N. Srinivasa, "Vision-based vehicle detection and tracking method for front collision warning in automobiles," in *Proc. IEEE Intelligent Vehicles Symposium*, vol. 2, pp. 626–631, June 2002.
- [8] A. Shashua, Y. Gdalyahu, and G. Hayon, "Pedestrian detection for driving assistance systems: Single-frame classification and system level performance," in *Proc. IEEE Intelligent Vehicles Symposium*, pp.1-6, 2004.
- [9] Y. Ma, S. Soatto, J. Kosecka, S. S. Sastry, *An invitation to 3-D vision*, Springer, 2000.
- [10] A. Benshair, A. Bertozzi, A. Broggi, A. Fascioli, S. Mousset, and G. Toulminet, "Stereo vision-based feature extraction for vehicle detection," in *Proc. IEEE Intelligent Vehicles Symposium*, pp. 465–470, June 2002.
- [11] G. Toulminet, M. Bertozzi, S. Mousset, A. Benshair, and A. Broggi, "Vehicle detection by means of stereo vision-based obstacles features extraction and monocular pattern analysis," *IEEE Trans. on image processing*, vol. 15, no. 8, pp. 2364–2375, August 2006.
- [12] N. Hautière, R. Labayrade, and D. Aubert, "Real-time disparity contrast combination for onboard estimation of the visibility distance," *IEEE Trans. on intelligent transportation systems*, vol. 7, no. 2, pp. 201–212, June. 2006.
- [13] C. Caraffi, S. Cattani, and P. Grisleri, "Off-road path and obstacle detection using decision networks and stereo vision," *IEEE Trans. on intelligent transportation systems*, vol. 8, no. 4, pp. 607–618, Dec. 2007.
- [14] <http://www.citr.auckland.ac.nz/6D/datasets.htm>